JOURNAL OF Materials CHEMISTRY

Synthesis and spectroscopic characterisation of Y-doped Cd_2SnO_4

Antonino Gulino and Ignazio Fragalà

Dipartimento di Scienze Chimiche Università di Catania, V.le A. Doria 6, 95125 Catania, Italy

Received 4th May 1999, Accepted 10th September 1999

Y-Doped cadmium oxide has been prepared by a solid state reaction of CdO and Y_2O_3 in air, and by a coprecipitation procedure starting from CdO and $Y(NO_3)_3{\cdot}6H_2O$. Y-Doped dicadmium stannate has been synthesised by firing well blended mixtures of Y-doped CdO and SnO_2 in air. Both Y-doped CdO and Cd_2SnO_4, have been characterised by XRD, IR, EPR and XPS. XRD measurements confirm the presence of single cubic CdO and orthorhombic Cd_2SnO_4 phases. EPR analysis suggests an increased concentration of conduction electrons and electron mobility upon 2% Y-doping. IR specular reflectance spectra show enhanced reflectivity in the mid IR for Y-doped Cd_2SnO_4 samples. XPS measurements highlight yttrium segregation to the sample surface.

1 Introduction

Both cadmium oxide, CdO, and dicadmium stannate, Cd_2SnO_4, exhibit interesting electronic and optical properties which have been widely investigated owing to their potential use as photosensitive anode materials for photochemical cells and other solar energy applications.[1–16] In these compounds cadmium interstitials or intrinsic oxygen vacancies act as n-type defects thus producing donor states in the bulk bandgap and promoting electronic conduction.[17–23]

Different amounts of defects, introduced depending on the synthesis procedure, strongly affect the electronic and spectroscopic properties of these two compounds.[7,20] In fact, synthesis under oxidising conditions yields yellow compounds, whilst in a reducing atmosphere green compounds, with higher carrier concentrations, are obtained.[7,20] The synthesis and characterisation of CdO and Cd_2SnO_4 have been the subjects of extended studies.[24]

^{113}Cd NMR, EPR, ^{119}Sn Mössbauer, XRD, EELS, UPS, optical, electrical and photoelectrochemical measurements have been performed to characterise polycrystalline and single crystal samples of C_2SnO_4.[1–27] The results obtained are indicative of the presence in the green phase of a concentration of conduction electrons which is higher than that found in the yellow phase.[5,18–20] Nevertheless, lower electrical conductance, due to lower electron mobility, has been observed in the green phase.[5,18–20] Moreover, it has been reported that the photoelectrochemical properties of polycrystalline Cd_2SnO_4 are better than those of single crystal samples, possibly because of a lower concentration of oxygen vacancies in the latter.[13] Besides, films of Cd_2SnO_4 exhibit resistivities which increase with decreasing thickness.[11]

In addition, EPR studies of single crystals and pressed powders of CdO, fired at high temperatures, provided evidence of metal based (Cd 5s) conduction electrons, together with Cd^+ ions where the unpaired electron was partly on the central Cd^+ ion but reaching far out into the crystal.[28] Cd^+ ions, present in significant amounts in samples fired at 1000 °C, did not appear associated with conduction band properties.[17,28] Obviously chemical doping represents another convenient way to increase conduction electrons and both CdO and Cd_2SnO_4 have been doped with different cations.[5,17–20] For example, both In- and Sb-doped Cd_2SnO_4 have revealed that dopants enhance the number of metal based (Cd 5s) conduction electrons even though the conduction band structure seems to be less affected.[18–20]

Finally, increased light transparency in the UV and reflectance in the IR regions, which depends upon the carrier concentration, accompany enhanced conductivity.[2,3,11,15,20,26,27,29]

In the present study we report on the synthesis and spectroscopic characterisation of yttrium-doped Cd_2SnO_4, in order to provide further insight into the semiconductor properties of this material and to check the influence of rare earth doping.

2 Experimental details

Cadmium oxides are exceedingly toxic, therefore care was taken during sample manipulation.

Y-Doped cadmium oxide ($Cd_{1-x}Y_xO$) ($1 \leqslant x \leqslant 0.05$) sample powders were synthesised following two different procedures. Procedure **a** involved firing of a well blended mixture of appropriate quantities of the starting grade oxides (CdO and Y_2O_3, Aldrich 99.99%).[17] Procedure **b** involved a coprecipitation method using yttrium nitrate hexahydrate [$Y(NO_3)_3{\cdot}6H_2O$] and CdO. In this case, appropriate quantities of the starting materials were separately dissolved in water [$Y(NO_3)_3{\cdot}6H_2O$] and in concentrated HCl (CdO). Their solutions were mixed together and, under continuous stirring, neutralised with Na_2CO_3.[12] The hydroxides thus formed were filtered off, washed with distilled water and dried at 90 °C. Powders resulting from both procedures, and some undoped CdO, were fired in air for 7 days at 880 °C. Polycrystalline undoped and Y-doped Cd_2SnO_4 sample powders were synthesised by thermal reaction, in air at 1050 °C for 6 hours, of mixtures of the reagent grade oxide ($Cd_{1-x}Y_xO$ and SnO_2 with $0 < x \leqslant 0.02$) in the correct stoichiometric proportions and slowly cooled to room temperature.[24] All thermal treatments were performed in recrystallised alumina crucibles with closely fitting lids.[24] Undoped Cd_2SnO_4 powders are yellow, whilst the Y-doped Cd_2SnO_4 analogues are yellow-green because of some reduction of Sn^{IV} to Sn^{II}.[7] Sample powders of both undoped and Y-doped Cd_2SnO_4 were pressed into pellets (10 MPa) between tungsten carbide dies (13 mm) and then fired for 8 hours in air at 900 °C.[20]

The phase composition of the products was monitored by X-ray diffraction (XRD), using a computer interfaced Philips PW 1130 diffractometer operating in a Bragg–Brentano geometry (Cu-Kα radiation, 25 mA and 40 kV) over the angular range $20° < 2\theta < 80°$ (0.02° stepsize) with a 20 s channel^{-1} dwell time.[30]

EPR spectra of weighed amounts of finely ground sample powders were obtained using a Bruker ER 200D instrument driven by the ESP 3220 data system. All spectra were recorded at room temperature. Care was taken over the position of the sample with respect the resonance cavity in order to perform analyses of different samples under identical instrumental conditions. Results were always highly reproducible. The diphenylpicrylhydrazyl (dpph) radical ($g=2.0036$) was used to standardise the klystron frequency, the magnetic field being monitored by a Bruker ER 035M gauss meter.[31] The values of EPR peak area/grams ratios (hereafter IPAG) of different samples were obtained by integration of the EPR signals (ESP 3220 data system). EPR peak widths were estimated from the separation between the maximum slope points in the derivative spectra.[5]

IR specular reflectance spectra were measured using unpolarised radiation incident at 45° to the surface normal in a Perkin Elmer 1710 FTIR spectrometer in the range 400–4000 cm^{-1}.[29] The experimental resolution was set at 2 cm^{-1}. Background interferograms were recorded from an aluminium mirror, assumed to be 100% reflecting over the region of interest.[29]

X-Ray photoelectron spectroscopy (XPS) measurements were performed on pellets with a PHI 5600 Multi Technique System (operating in the 10^{-10} Torr pressure regime) using unmonochromated Al-Kα radiation. The spectra were taken at 45° relative to the surface plane. Resolution, correction for satellite contributions and background removal have been described elsewhere.[30] No sample manipulation was done (such as argon ion etching or vacuum annealing) in order to analyse samples under identical conditions (as obtained) with all techniques. The remaining adventitious carbon contamination of the surfaces (284.6 eV binding energy) gave a measured C 1s/O 1s XPS intensity ratio of around 5/100.

3 Results and discussion

3.1 XRD analysis

XRD data indicate that both undoped and Y-doped CdO brown samples consist of the expected single cubic phase with the lattice parameter in good agreement with the literature when $x \leqslant 3.5\%$ (ASTM 5-0640).[17,32] Beyond this doping level, reflections of cubic Y_2O_3 (ASTM 5-0574)[32] begin to appear thus suggesting that the solubility limit of Y in CdO has been exceeded ($T=880$ °C). Both undoped and Y-doped Cd_2SnO_4 show a single phase with an orthorhombic unit cell (ASTM 20-0188).[32–34]

Crystal sizes of both Y-doped CdO and Cd_2SnO_4 were determined from XRD data using the Scherrer and Warren equation: $S=0.9\lambda/(B\cos\theta_B)$.[35] The resulting values of crystallite sizes, reported in Tables 1 and 2, are in the range 63–81 nm for Y-doped CdO and 81–95 nm for Y-doped Cd_2SnO_4. No significant variations in crystal sizes were observed for samples **b**. Pellets gave XRD patterns identical to those of unpressed powders.

3.2 EPR analysis

Relevant experimental observations on CdO samples are summarised in Table 1.

Fig. 1(a) shows the EPR spectrum of a representative 2% Y-doped CdO sample **a**. In particular two peaks are always observed with g values of 1.86 ± 0.01 and 1.99 ± 0.01 and peak widths of 93 and 52 G respectively. Both g and peak width values are similar to those of impure CdO semiconductors fired up to 1000 °C.[28] Therefore the signal with $g=1.86$ can be safely assigned to conduction band electrons. This g value is somewhat higher than that previously reported (1.78).[28] The peak at $g=1.99$, in agreement with literature data,[28] is due to Cd^+ on the site of a Cd^{2+} ion.[28] Cd^+ ions arise from polaronic self-trapping of electrons introduced by oxygen deficiency at Cd^{2+} sites to generate localised $5s^1$ states which are not involved in the conduction band.[28] Similar behaviour has been previously described for other systems, *i.e.* TiO_2 where self-trapped electronic states are observed close to the conduction band edge rather than in the middle of the band gap.[36] In addition, a decrease in peak widths upon increasing the Y-doping level has been observed, with widths of the 2% Y-doped sample being the lowest observed so far. Broader EPR signals were always detected for samples **b**.

Fig. 1(b) shows the EPR spectrum of a representative 2% Y-doped Cd_2SnO_4 sample **a**. All present EPR spectra of undoped and Y-doped Cd_2SnO_4 show an intense peak with a g value of 1.85 ± 0.01 which does not vary with the Y-doping level, synthesis procedure, or intensity of the resonance (Table 2). This value is almost identical to that previously reported for undoped Cd_2SnO_4 and the resonance arises from the conduction electrons.[7]

The intensity of the EPR conduction electron resonance is a function of the number of conduction electrons.[7] In this context, an interesting trend of the IPAG values is obtained. In particular the concentration of conduction electrons in samples **a** significantly increases on passing from undoped Cd_2SnO_4 to 1 and 1.5% Y-doped analogues, whilst a dramatic fall-off is observed for 2% Y-doped Cd_2SnO_4 (Table 2). At variance, both 1 and 2% Y-doped samples **b** show higher IPAG values than the undoped samples, with the IPAG value for the 1% doped sample again being higher than that of the 2% Y-doped sample. This behaviour suggests that procedure **b** is more effective in enhancing the carrier concentration than procedure **a**.

Previous studies on air-annealed Sb-doped Cd_2SnO_4 have shown a linear relationship between the EPR peak width and the Sb nominal doping level.[5] The EPR peak width depends on the electron spin relaxation process efficiency which, in conducting samples, may be related to electron mobilities.[5] Therefore, the increasing Sb concentration parallels an increased number of conduction electrons having, however, decreased electron mobility due to electron scattering by donors, which increases as a function of the donor concentration.[5] Note that the EPR peak widths observed in all the present Y-doped Cd_2SnO_4 samples are always smaller than those observed for the Sb-doped analogues, thus suggesting higher electron mobilities.[5] Moreover the width observed for 2% Y-doped Cd_2SnO_4 **a** samples (20 G) represents the lowest

Table 1 Crystal sizes and EPR parameters of Y-doped CdO[a]

Nominal Y-doping level (atom%)	Crystal size/nm	g-Value	Peak width/G
0 (commercial)	119	1.82, 2.00	121, 175
0 (7 days at 880 °C)	81	1.82 weak signal, 1.99	147
1	71	1.87 (1.88), 2.00 (not resolved)	108 (174), 86 (not resolved)
1.5	63	1.86, 1.99	104, 61
2	81	1.86 (1.88), 1.99 (1.92)	93 (not resolved), 52 (not resolved)
5	80	(1.89), (2.01)	(128), (95)

[a]Values in parentheses refer to samples **b**.

Table 2 EPR and resistivity parameters of Y-doped Cd_2SnO_4[a]

Nominal doping level (atom%)	Crystal size/nm	*g*-Value	Peak width/G	IPAG[b]	Resistivity/Ω cm^{-2}
0	71	1.84	26	1	38
1	95	1.85 (1.85)	29 (34.3)	2.6 (5)	27 (37)
1.5	85	1.85	26	3.5	32
2	81	1.85 (1.86)	20 (42.9)	0.15 (4.7)	7 (75)

[a]Values in parentheses refer to samples **b**. [b]Values have been normalised to the value observed for undoped Cd_2SnO_4.

value within the present samples. This fact should allow one to forecast higher conductivity for 2% Y-doped Cd_2SnO_4 relative to the undoped and 1–1.5% Y-doped analogues.

In the case of Y-doped CdO samples, the observed monotonous decrease in peak widths upon increasing the Y-doping level up to 2 atom% is in good agreement with previously reported data.[17] In fact, it has been demonstrated that the carrier concentration increases linearly with the doping level because of the substitution of Y^{III} on Cd^{II} sites.[17] In addition, the surface plasmon peak moves progressively to higher loss energy as the bulk dopant content increases, the highest value being 0.66 eV.[17] Moreover, a well defined conduction band feature appears in He-I UPS spectra of doped samples; this feature is associated with a shift of the valence band edge towards high binding energy.[17] All these observations suggest that Y acts as an effective n-type dopant for CdO.

Samples **b** show EPR peak widths (Table 2) which are larger than those of samples **a**.

It has been reported that particle size effects may influence the EPR peak widths.[5] Previous work on doped SnO_2 and on many other closely related systems have indicated that dopants influence grain sizes, since they segregate to the surface, thus affecting grain growth.[29] As a consequence EPR skin effects, which are particle size dependent, could be the origin of this phenomenon.[5] In the present case, 1% Y-doped Cd_2SnO_4 shows crystal sizes of 95 nm, somewhat larger than those shown by the 1.5 and 2% doped samples (85 and 81 nm respectively, Table 2). Therefore, the skin effects should be similar in 1.5 and 2% doped samples, thus permitting some comparisons.

3.3 FTIR analysis

IR specular reflectance analysis is an effective technique for the investigation of surface conductivity of ceramic oxides.[29] The IR specular reflectance spectrum of polycrystalline undoped Cd_2SnO_4 represents a superposition of structures due to allowed vibrations with two distinct maxima in the 500–600 cm^{-1} region (Fig. 2). Y-Doping has a profound effect on the reflectance spectra, as the increased number of free carriers screens out coupling between the external electromagnetic fields and the electric fields associated with the IR-active phonons. In fact all Y-doped Cd_2SnO_4 samples show enhanced reflectivity in the mid-IR (Fig. 2) above the phonon frequencies, where the undoped material is less reflecting. Note that the reflectivity parallels the IPAG values. In particular a strong increase in reflectivity is observed on passing from undoped to 1% Y-doped samples **a**. Accordingly, the IPAG value goes from 1 to 2.6. Moreover, a significant further increase of the IPAG value is associated with a sizeable increase of the reflectivity in 1.5% doped samples. The dramatic fall-off of the IPAG value observed for 2% Y-doped Cd_2SnO_4 (Table 2) is, therefore, consistent with the lowest reflectivity observed in the present Y-doped **a** materials. Minor variations are observed with samples **b**. In fact, both 1 and 2% Y-doped systems show high reflectivity, with that of the 2% doped system only slightly smaller than that of the 1% doped sample. In accordance, high IPAG values are found, with, once more, that of the 2% doped sample somewhat smaller than that of the 1% doped sample. Again, it transpires that procedure **b** is more efficient in increasing the carrier concentration.

The IR results are in good agreement with some, admittedly limited, room temperature resistivity measurements of typical

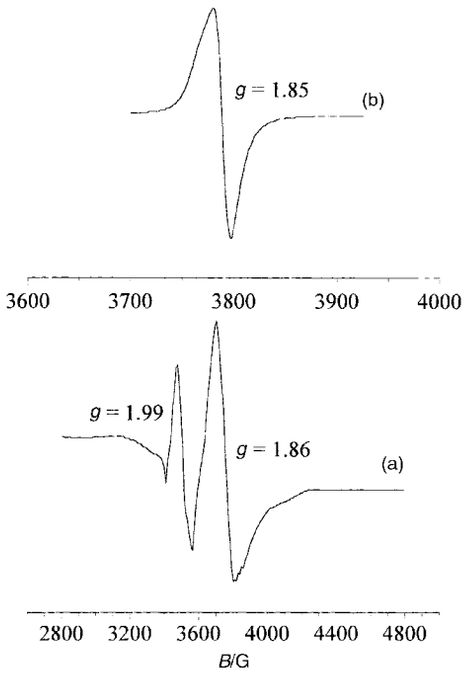

Fig. 1 EPR spectra of representative 2% Y-doped CdO (a) and Cd_2SnO_4 (b) **a** samples.

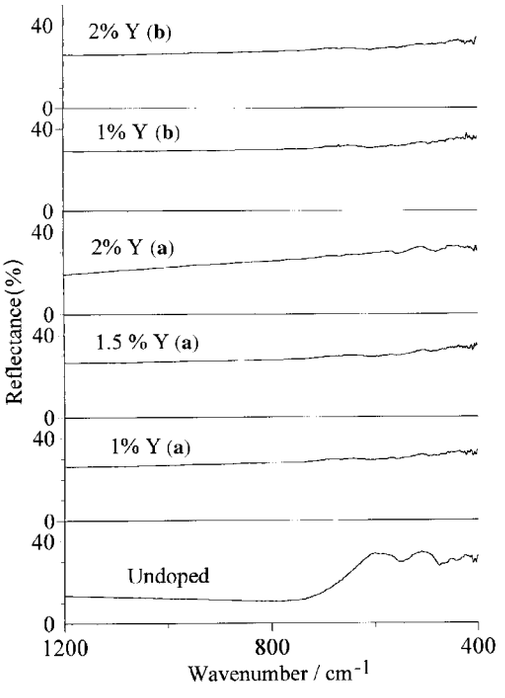

Fig. 2 IR specular reflection spectra of undoped and Y-doped Cd_2SnO_4. Letters in parentheses refer to the synthesis procedure.

13 mm ceramic pellets between two point contacts at opposite edges, for which small but significant variations have been observed upon doping. Thus, the resistance of undoped yellow Cd_2SnO_4 was 38 Ω, in good agreement with previously reported values.[7] Lower values were exhibited by Y-doped green pellets. Note that the 2% Y-doped Cd_2SnO_4 sample **a** shows the lowest IPAG value (0.15), the lowest EPR peak width (20 G), the lowest resistivity (7 Ω) and the lowest IR reflectivity within the Y-doped samples, whilst the 1.5% Y-doped Cd_2SnO_4 sample **a** shows the largest IPAG value (3.5), an EPR peak width larger than that of the 2%, the largest resistivity (32 Ω) and the largest IR reflectivity within the Y-doped samples. By contrast, upon varying the doping level samples **b** always show larger EPR peak widths, larger and almost constant IPAG values, larger resistivity and larger IR reflectance.

3.4 XPS measurements

Fig. 3 shows the Al-Kα XPS of 1% Y-doped Cd_2SnO_4 **a** pellets in the Cd, Sn and Y 3d binding energy (BE) region. Note that the observed BEs for Cd ($3d_{5/2}=404.1$ and $3d_{3/2}=411.0$ eV) and Sn ($3d_{5/2}=485.4$ and $3d_{3/2}=493.8$ eV) are identical to those of undoped Cd_2SnO_4.[20] No variation of BEs was observed for Cd 3d, Sn 3d, and O 1s levels upon increasing the Y-doping level. The Y 3d feature (Y $3d_{5/2}=156.0$ eV) is strongly reminiscent of that previously reported for Y-doped CdO, often encountered with yttrium oxides and Y-doped ZrO_2 powders.[17,37,38] The XPS results have been used to quantify the cation surface distribution making due allowance for the atomic sensitivity factors.[39] The surface Sn/Cd ratio is 0.48 ± 0.05 for undoped Cd_2SnO_4 pellets, very close to the theoretical value, and shows a monotonous increase upon increasing the Y doping level (0.50, 0.52 and 0.64 for 1, 1.5 and 2% Y-doped Cd_2SnO_4 respectively). The intensity of the Y 3d peak, at all the doping levels investigated, is much greater than expected on the basis of the nominal doping, the Y/Cd ratio being 0.76 for 1% Y-doped Cd_2SnO_4. This observation indicates a pronounced segregation of yttrium to the surface thus resulting in a new surface phase (Y_2O_3) which does not contribute electrons to the conduction band.[17,36,40,41]

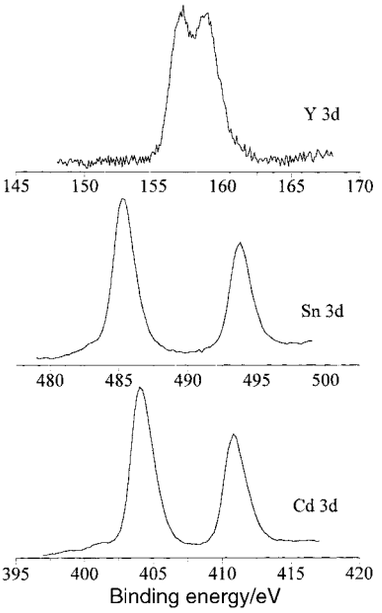

Fig. 3 Al-Kα excited XPS normal emission of a representative 1% Y-doped Cd_2SnO_4 **a** sample measured in the Cd–Sn–Y binding energy regions. Structure due to satellite radiation has been subtracted from the spectra.

4 Conclusion

Y-Doped Cd_2SnO_4, has been synthesised and characterised by XRD, IR, EPR, XPS and simple resistivity measurements. XRD measurements confirm the presence of single orthorhombic Cd_2SnO_4 phases. Both EPR results and IR specular reflectance spectra are indicative of increased carrier concentration in Cd_2SnO_4 samples **a** upon light Y-doping (1–1.5%). Simple resistivity measurements indicate lower resistivities in Y-doped Cd_2SnO_4 **a** samples with respect to the undoped analogues.

The key to understanding this behaviour may be in analysing the mode of bulk Y^{3+} substitution. Three possible limiting modes of bulk substitution warrant consideration. The first involves Y^{3+} on Cd^{2+} sites with donation of the extra valence electron provided by Y into the conduction band. This, in the absence of other effects such as scattering between donors,[5,18–20] would lead to significantly enhanced conductivity. The second alternative involves Y^{3+} on Sn^{IV} sites. In this case there will be some suppressing of the intrinsic conductivity of Cd_2SnO_4 itself because Y^{3+} behaves as an acceptor. The third mode involves Y^{3+} in both Cd^{2+} and Sn^{IV} sites. This time both previous mechanisms are operating. It is therefore evident that a delicate balance between donors, acceptors and scattering of carriers determines the conduction properties.

Therefore the 2% Y-doped Cd_2SnO_4 sample **a**, which shows the lowest IPAG value (0.15), the lowest EPR peak width (20 G) the lowest resistivity (7 Ω) and only a moderate increase in IR reflectivity, with respect to the undoped samples, represents the case in which Y^{3+} substitutes for both Cd^{2+} and Sn^{IV} and the obtained donor concentration is likely to minimise scattering by carriers thus increasing the conductivity.

Acknowledgements

We are indebted to Professor R. P. Bonomo for the use of the EPR spectrometer and for helpful discussion of the EPR results. Moreover Dr. G. Baratta, Osservatorio astrofisico, Università di Catania, is acknowledged for FTIR measurements. I. F. and A. G. thank the MURST and the CNR (Rome) for financial support.

References

1 W. Xiaochun, W. Rongyao, Z. Bingsuo, W. Li, L. Shaomei, X. Jiren and H. Wei, *J. Mater. Res.*, 1998, **13**, 604.
2 X. Wu, T. J. Couts and W. P. Mulligan, *J. Vac. Sci. Technol. A*, 1997, **15**, 1057.
3 T. J. Couts, X. Wu, W. P. Mulligan and J. M. Webb, *J. Electron. Mater.*, 1996, **25**, 935.
4 R. Dragon, S. Wacke and T. Gorecki, *J. Appl. Electrochem.*, 1995, **25**, 699.
5 K. J. D. MacKenzie, C. M. Cardile and R. H. Meinhold, *J. Phys. Chem. Solids*, 1991, **52**, 969 and references therein.
6 T. Hashemi, C. H. Hogarth and F. Golestani-Fard, *J. Mater. Sci.*, 1988, **23**, 2645.
7 C. M. Cardile, R. H. Meinhold and K. J. D. MacKenzie, *J. Phys. Chem. Solids*, 1987, **48**, 881.
8 C. M. Lambert, *Sol. Energy Mater.*, 1981, **6**, 1.
9 D. E. Hall, *J. Electrochem. Soc.*, 1980, **127**, 308.
10 F. P. Koffyberg and F. A. Benko, *Appl. Phys. Lett.*, 1980, **37**, 320.
11 N. Miyata, K. Miyake, K. Koga and T. Fukushima, *J. Electrochem. Soc.: Solid-State Sci. Technol.*, 1980, **127**, 918.
12 K. J. D. MacKenzie, W. A. Gerrard and F. Golestani-Fard, *J. Mater. Sci. Lett.*, 1979, **14**, 2509.
13 K. J. D. MacKenzie, W. A. Gerrard and F. Golestani-Fard, *Silic. Ind.*, 1979, **4–5**, 97.
14 G. Haacke, W. E. Mealmaker and L. A. Siegel, *Thin Solid Films*, 1978, **55**, 67.
15 G. Haacke, H. Ando and W. E. Mealmaker, *J. Electrochem. Soc.: Solid-State Sci. Technol.*, 1977, **124**, 1923.
16 A. J. Nozik, *Phys. Rev. B*, 1972, **6**, 453.

17 Y. Dou, R. G. Egdell, T. Walker, D. S. L. Law and G. Beamson, *Surf. Sci.*, 1998, **398**, 241.
18 Y. Dou and R. G. Egdell, *Surf. Sci.*, 1997, **372**, 289.
19 Y. Dou and R. G. Egdell, *Surf. Sci.*, 1997, **377–379**, 181.
20 Y. Dou and R. G. Egdell, *J. Mater. Chem.*, 1996, **6**, 1369.
21 F. P. Koffyberg, *Solid State Commun.*, 1971, **9**, 2187.
22 R. Haul and D. Just, *J. Appl. Phys.*, 1962, **33**, 487.
23 A. Cimino and M. Marezio, *J. Phys. Chem. Solids*, 1960, **17**, 57.
24 C. M. Cardile, *Rev. Solid. State Sci.*, 1991, **5**, 31.
25 R. Pis Diez, E. J. Baran, A. E. Lavat and M. C. Grasselli, *J. Phys. Chem. Solids*, 1995, **56**, 135.
26 M. S. Setty, *J. Mater. Sci. Lett.*, 1987, **6**, 909.
27 F. Golestani-Fard, C. A. Hogarth and D. N. Waters, *J. Mater. Sci. Lett.*, 1983, **2**, 505.
28 R. H. Meinhold, *J. Phys. Chem. Solids*, 1987, **48**, 927.
29 R. G. Egdell, A. Gulino, C. Rayden, G. Peacock and P. A. Cox, *J. Mater. Chem.*, 1995, **5**, 499.
30 A. Gulino, S. La Delfa, I. Fragalà and R. Egdell, *Chem. Mater.*, 1996, **8**, 1287.
31 R. P. Bonomo, E. Conte, G. De Guidi, G. Maccarrone, E. Rizzarelli and G. Vecchio, *J. Chem. Soc., Dalton Trans.*, 1996, 4351.
32 American Society for Testing and Material, Powder Diffraction Files, Joint Committee on Powder Diffraction Standards, USA, Set 1–5 Revised, Inorganic, 1974.
33 M. Von Tromel , *Z. Anorg. Allg. Chem.*, 1969, **371**, 237.
34 R. D. Shannon, J. L. Gillson and R. J. Bouchard, *J. Phys. Chem. Solids*, 1977, **38**, 877.
35 B. E. Warren, *X-Ray Diffraction*, Addison-Wesley, Reading, MA, 1969.
36 A. Gulino, A. E. Taverner, S. Warren, P. Harris and R. G. Egdell, *Surf. Sci.*, 1994, **315**, 351 and references therein
37 D. Majumdar and D. Chatterjee, *J. Appl. Phys.*, 1991, **70**, 988.
38 A. E. Hughes, *J. Am. Ceram. Soc.*, 1995, **78**, 369.
39 D. Briggs and M. P. Seah, *Practical Surface Analysis*, Wiley, Chichester, 1994, 2nd edn.
40 R. G. Egdell and S. C. Parker, in *Science of Ceramic Interfaces*, ed. J. Nowotny, Material Science Monographs no. 75, Elsevier, Amsterdam, 1991, p. 41, and references therein.
41 W. C. Mackrodt and P. W. Tasker, *J. Am. Ceram. Soc.*, 1989, **72**, 1576.

Paper 9/03480C